Numerical Study of Aerodynamic Force and Surface Pressure of Square Prism in a Uniform Flow

Takeshi Ishihara[a], Shinichi Oka[b]

a Associate Professor, University of Tokyo, 7-3-1, Hongo, Bunkyo-ku, Tokyo, 101-0023, Japan
b Fluent Asia Pacific Co. Ltd., 6-10-1, Nishishinjuku ,Shinjuku-ku, Tokyo 160-0023, Japan

KEYWORDS: Aerodynamic force, surface pressure, square prism, separated flow, CFD, LES

ABSTRACT: Aerodynamic features of square prism with respect to various angles of attack were investigated using Large Eddy Simulation (LES) turbulence model. The results met well with experiment data in time average aerodynamic characteristics, drag force coefficients, lift force coefficients, and surface pressure coefficients for all cases examined in this study. In conclusion, the numerical approach successfully predicts mean aerodynamic features of square prism whereas further investigation is necessary for the prediction of fluctuating values.

1 INTRODUCTION

To know aerodynamic features around bluff bodies is important in wind engineering area such as galloping problems often seen in electric power lines. From the past experiments[1, 2], aerodynamic characteristics around a rectangular cylinder depend on angle of attack to a flow. Particularly, aerodynamic forces, drag, lift, and moment, and surface pressure dramatically change when a separated flow at front edge reattaches to the side of body [1), 2)]. Many numerical studies have been accomplished in this area, and successful to some extent. For example, Hirano et.al.[3] showed prediction of flow around 2:1 rectangular cylinder using LES turbulence model resulting good agreement with experiments on mean drag force, mean lift force, and Strouhal number, however, fluctuations, important when aeroacoustics is of interest, were not included in the discussion. LES, a turbulence model that calculates large eddies directly while models small eddies, captures inherent turbulence properties of unsteady and three dimensional characteristics. LES seems to be one of the suitable prediction approaches on this issue.

Regarding square prism, many researches have performed and examined for 0 degree attack angle case, however, few have focused on variations of attack angles and discussion on fluctuations. For example, Tamura[4] predicted mean drag forces and mean lift forces for various attack angles using DNS, and got good agreement with experimental data, but no discussion on fluctuations was presented. Fluctuating forces are important for identifying and quantifying sound source generated by bluff bodies, and for evaluating correlation of turbulence length[5]. Taylor et.al.[6] have tried predicting fluctuations with respects to various attack angles using vortex method, however, the results did not meet well with experiments.

In summary, few researches have been accomplished for predicting aerodynamic characteristics of flow around square prism including fluctuations with respect to various angles of attack.

In this study, aerodynamic features of square prism in a uniform flow with respect to various angles of attack were investigated by LES approach. The results were compared with experiments and examined to evaluate if this approach can be used for predictions such as the galloping and aeroacoustics problems.

2 NUMERICAL MODEL

LES turbulent model, in which small eddies are modeled whereas large eddies are directly calculated, was used for the calculations. Advantage of LES is that the model captures turbulence characteristics that are unsteady and three dimensional in nature.

2.1 *Basic Equations*

Basic equations, filtered incompressible Navier-Stokes equations in space, are shown below;

$$\frac{\partial \rho \bar{u}_i}{\partial x_i} = 0$$

$$\frac{\partial}{\partial t}(\rho \bar{u}_i) + \frac{\partial}{\partial x_j}(\rho \bar{u}_i \bar{u}_j) = \frac{\partial}{\partial x_j}\left(\mu \frac{\partial \bar{u}_i}{\partial x_j}\right) - \frac{\partial \bar{p}}{\partial x_i} - \frac{\partial \tau_{ij}}{\partial x_j}$$

Where, $\bar{u}_i$ and $\bar{p}$ are filter averaging velocity and pressure respectively. ρ is fluid density, and μ is fluid viscosity. τ_{ij} is sub-grid scale Reynolds stress defined by the following equation;

$$\tau_{ij} \equiv \overline{\rho u_i u_j} - \rho \bar{u}_i \bar{u}_j$$

Because sub-grid scale stress, derived by the filtered operation, is unknown, we use the following eddy viscosity model to close the equations.

$$\tau_{ij} = -2\mu_t \bar{S}_{ij} + \frac{1}{3}\tau_{kk}\delta_{ij}$$

Where, μ_t is sub-grid turbulence viscosity, $\bar{S}_{ij}$ is rate of strain tensor for the resolved scale.

2.2 *Smagorinsky Model*

Smagorinsky model[8] is used for sub-grid scale turbulence viscosity μ_t as follows;

$$\mu_t = \rho L_s^2 |\bar{S}| \quad |\bar{S}| \equiv \sqrt{2\bar{S}_{ij}\bar{S}_{ij}}$$

L_s is the sub-grid scale mixing length, $L_s = \min(\kappa d, C_s V^{1/3})$
Where, κ is von Kármán constant, κ =0.42, d is the distance to the closest wall, V is the volume of the computer cell. C_s is Smagorinsky constant, in which 0.1 is widely used, however, in this calculation, 0.032 was used that stems from previous study[9].

2.3 *Numerical Approach*

Unstructured finite volume method using collocated grid was used for the calculation. Second order central difference scheme for convective term and the second order difference scheme for unsteady term were used to discretize the basic equations to convert algebraic equations. SIMPLE method was used to solve the algebraic equations. FLUENT[10], a CFD software, is used as the solver.

3 MODELING CONDITIONS AND BOUNDARY CONDITIONS

3.1 *Model Parameters and Boundary Conditions*

Figure 1 shows calculation domain and mesh used for the model. The length of each prism edge, D, is 1cm. Span length L is 1cm. Width and the length of the calculation domain are both 60 cm

In-flow velocity U is 15 m/s. The wall shear stress is obtained from the laminar stress-strain relationship as shown bellow;

$$\frac{\bar{u}}{u_\tau} = \frac{\rho u_\tau y}{\mu}$$

Outflow boundary condition was used at outlet boundary. Symmetry condition was used for both sides and top/bottom walls. 62 meshes were used for the square prism edge, and equally distributed 10 meshes were used in span wise direction. Smaller meshes were generated at each edge corner to avoid singularity of the solutions. Total number of cell is 175,000. Table 1 shows model parameters used for the calculation. Twelve cases, attack angles, 0°, 2°, 6°, 8°, 10°, 12, ° 13°, 14°, 16°, 20°, 30°, and 45° were chosen for the calculations.

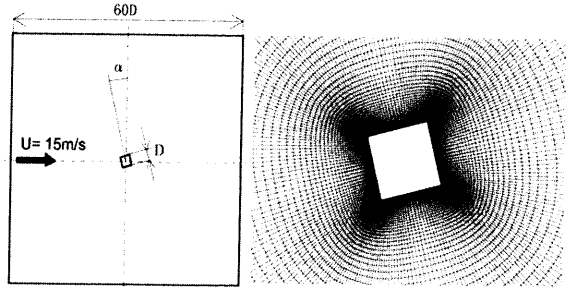

Figure 1. Calculation domain and mesh around square prism (at angle of attack α=14°)

Table 1. Model Parameters

Reynolds Number	10^4
Smagorinsky Coefficient Cs	0.032
Non dimensional time	0.03 D/U
No. of cells in span length	10
Total cell number	17500 x 10

3.2 *Definition of Coefficient of Surface Pressure and Non-dimensional Aerodynamic*

Surface pressure coefficient is defined as follows;

$$C_p = \frac{p - p_{ref}}{\frac{1}{2}\rho U^2_{ref}}, \qquad C_{pi}' = \sqrt{(C_{pi} - \bar{C}_{pi})^2}$$

Where, P_{ref} is the reference pressure located at lower edge inflow boundary with mid location in spanwise direction. ρ, 1.225kg/m^3, is reference density. Reference velocity, U_{ref}, is 15m/s that is the same as inflow velocity. Mean surface pressure coefficient, $\bar{C}_{pi}$, is derived by taking average of non-dimensional time over 100 to 300, then the values were taken average in spanwise direction. Time averaging procedure is the same for drag and lift force coefficients, C_d and C_l, presented later.

Mean drag coefficient and lift coefficients (C_d, C_l), and fluctuation drag coefficient and lift force coefficient (C_d', C_l') are defined as follows;

$$C_d = \overline{\sum_i C_{pi} A_i \cos\beta_i / A}\ ,\quad C_l = \overline{\sum_i C_{pi} A_i \sin\beta_i / A}$$

$$C_d' = \sqrt{\overline{\left(\sum_i (C_{pi} - \bar{C}_{pi}) A_i \cos\beta_i / A\right)^2}}\ ,\quad C_l' = \sqrt{\overline{\left(\sum_i (C_{pi} - \bar{C}_{pi}) A_i \sin\beta_i / A\right)^2}}$$

Where, A_i is area at ith cell of a square prism surface. A equals DL. β_i is an angle between flow direction and normal direction to the surface that include ith cell.

4 RESULTS

Mean and fluctuating drag and lift coefficients were calculated from the results of the simulations. Then we show the streamlines of the flow and surface pressure coefficients. Finally, those prediction results were compared to the experiments[1), 2)].

4.1 *Mean and fluctuation of Aerodynamic forces*

Fgure 2 shows mean drag coefficients C_d. As shown in Figure 2, angle of attack between α=0° and α=12°, C_d is moderately reduced whereas the curve becomes flat between α=12° and α=14°, followed by linearly increase of the value in the range between α=14° and α=30. C_d is moderately increase where α is greater than 30°. The predictions of C_d meet very well with experiment data except at α=0° where prediction is a little bit underestimated compared to experiment. Figure 3 shows mean lift coefficients C_l. As shown in the Figure 3, at angle of attack between α=0° and α=14°, C_l increases linearly as angle of attack increases. At around α=14°, C_l deceases moderately until α=30°, followed by flat between until α=45°. Overall, very good agreement is observed between the predictions and experiment data.

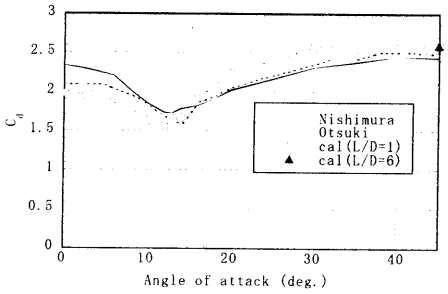

Figure 2 Mean drag coefficients

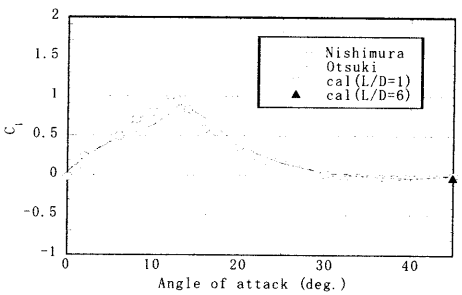

Figure 3 Mean lift coefficients

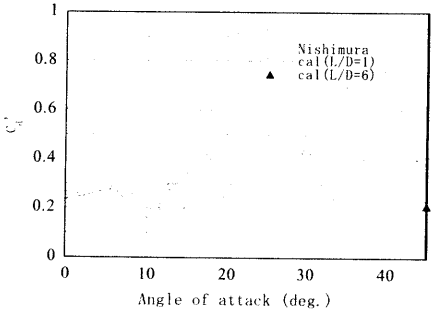

Figure 4 Fluctuation drag coefficients

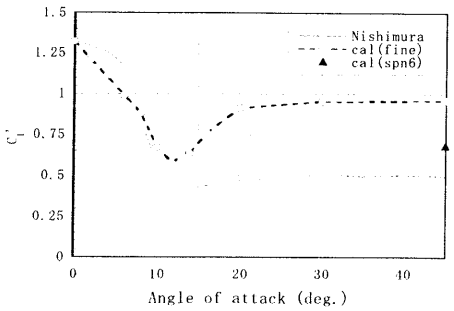

Figure 5 Fluctuation lift coefficients

Figure 4 shows fluctuation drag coefficients C_d'. C_d' curve is flat between α=0° and α=8°, followed by moderate reducing trend until α reaches to α=12°. The prediction results have good agreement with experiment in terms in qualitative point of view, however, in quantative point of

view, predictions are overestimated to some extent. C_d' increases where α is greater than 13°, and becomes flat where α is greater than 20°. However, no such increase at around α=14° is observed in the experiment data. Increase at around 13° in the predictions is clearly overestimated. Figure 5 shows fluctuation lift coefficients C_l'. As shown in Figure 5, where angle of attack is between α=0° and α=8°, C_l' is reduced steeply as angle of attack increased, followed by moderate decrease where α is greater than 12°. C_l' increases at angle greater than 14°, followed by flat where α is greater than 20°. According to the experiment, no such steep increase is observed where angle is greater than 14°, and predictions are clearly overestimated.

The reason that the predictions of C_d' and C_l' are overestimated is considered that spanwise length, L=1D, is too short to resolve breaking interaction of turbulence eddies that could reduce fluctuation of aerodynamic forces. Hayashi et.al.[11] reported that spanwise length affected fluctuation of arerodynamic forces, where C_l' was reduced to 1.39-0.96 when longer spanwise length were used, from L=2D to L=4D - 8D. In Figure 4 and 5, symbol of smeared plot at α=45° shows the case in L=6D. As presented in the Figure 5, significant improvement is observed particularly for fluctuation drag coefficient.

4.2 *Mean Flow Pattern*

Figure 6 shows time average streamline for α=0°, 8°, 14°, 20°, 30°, and 45°. As shown in Figure 6, at α=0°, flow separates at front edge, and no reattachment to the side face is observed. There are two large eddies behind the square prism. At α=8° flow separation forms eddies at both upper and lower faces. Eddies at lower face is larger than that of upper face eddies. There are non-symmetry eddies behind the square prism. Upper eddy is larger than lower eddy. At α=14°, one large eddy is formed behind square prism. At α=20°, in average, reattachment is presented at upper side face. Separation bubble is observed at front face edge. There are again two eddies formed behind the square prism. At α=30°, separation bubble becomes small, and shear layer always reattaches along with upper side face, then flow is separated at back edge. At α=45°, flow separates at side face near back edge corner. No separation at front edge is observed, and flow goes along with upper face. A couple of eddies are observed behind the square prism.

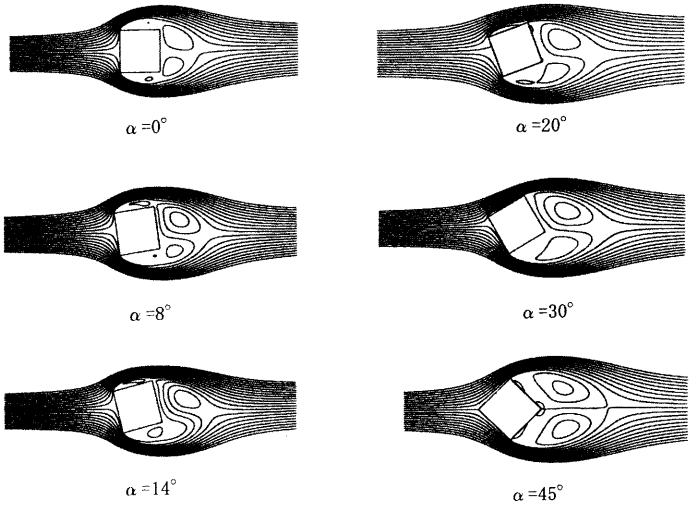

Figure 6 Time average streamlines at each angle of attack

4.3 *Pressure Coefficient Distributions*

Figure 7 shows mean surface pressure coefficients of both predictions and experiments for α=0°, 8°, 14°, 20°, 30°, and 45°. At α=0° between α=14°, overall pressure coefficients at upper side face reduce as angle of attack increases, and minimized at α=14°. At α=20°, a peak is observed that is caused by pressure recovery at upper side rear edge where reattachment of shear layer is supposed to be occurred. At α=30°, peak value at upper face becomes maximum, and reattachment occurs all the time. Negative pressure area where separation bubble exists is getting small. At α=45°, separation at front edge disappears and pressure at back face becomes small. As presented in the Figure 7, mean surface pressure coefficients meet very well with experiment data in all cases though small discrepancy is observed at α=0° that is consistent with the result that C_d is underestimated as shown in Figure 2.

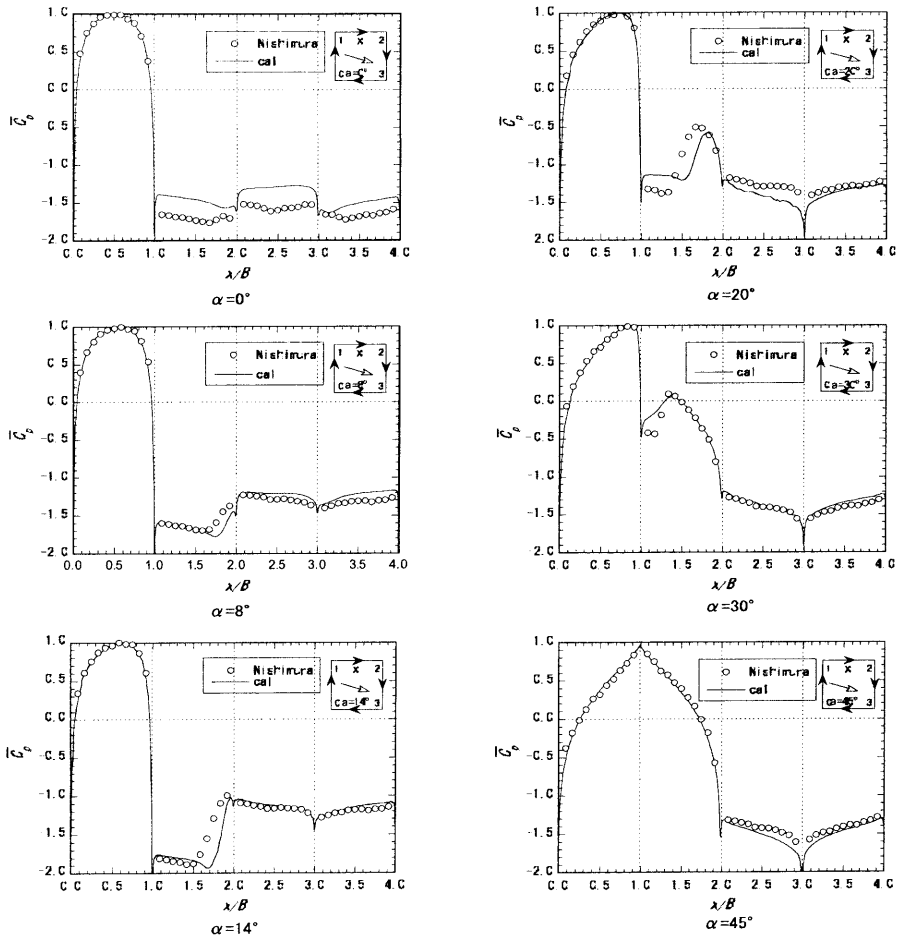

Figure 7 Mean surface pressure coefficients $\bar{C}_p$

Figure 8 shows fluctuation of surface pressure coefficients, C_p', of both predictions and experiments. As shown in Figure 8, at upper side face, fluctuation reduces as angle of attack increases. At α=0°, predictions relatively meet well with experiment compared to those at other angle of attack. At α=8°, prediction is clearly over estimated compared to the experiment data though good agreement is observed in terms of qualitative point of view. At α=14°, C_p' in the vicinity of back face close to upper side face increases whereas that of experiment reduces. The C_p' value is also overestimated. At α=20°, peak is observed at upper side face where reattachment is supposed to be occurred. Prediction of surface pressure at back face is overestimated. This is considered to be the reason that C_d' and C_l' are overestimated compared to those of experiment data. Similarly, predictions of C_d' and C_l' are overestimated at α=30° and 45°.

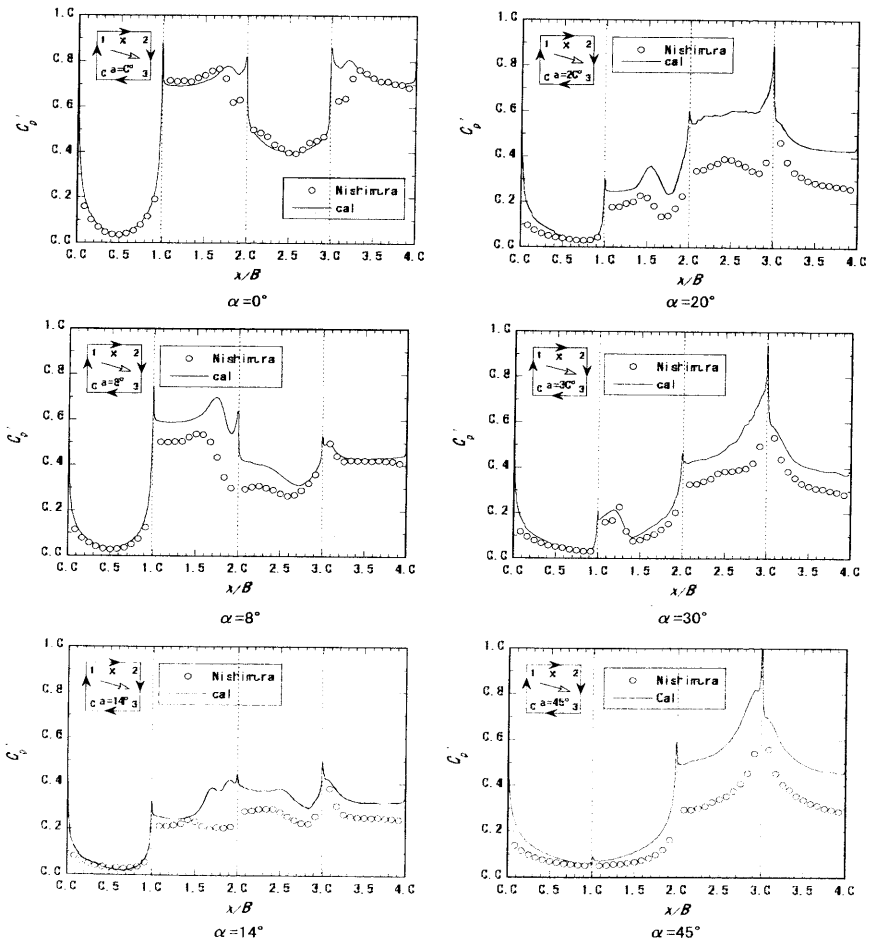

Figure 8 Fluctuations of surface pressure coefficients C_p'

5. CONCLUSIONS

Aerodynamic properties of square prism with respect to various angles of attack were predicted using LES turbulence model. The following is the summary of the study;

1) Regarding mean aerodynamics forces, C_d and C_l, the predictions met very well with the experiment except at α=20° where small discrepancy is observed C_d.
2) Regarding fluctuation aerodynamics forces, C_d' and C_l', the predictions met well with the experiment data where α=0° to 12° , however, for angle of attack α is greater than 20°, predictions were overestimated compared to experiment data though good agreements were observed qualitatively.
3) Significant improvement were observed by taking longer spanwise length, L/D=6 at α=45° that indicates that L=1D is too short to resolve turbulence eddies breaking interactions.
4) Regarding mean surface pressure, the prediction met very well with the experiment data though small difference is observed at α=0°.
5) Regarding fluctuation pressure coefficient, C_p', the results met well at α=0°, however, predictions of C_p' at back face were larger than that of experiment data, which caused overestimation of C_d' and C_l'.

This numerical approach successfully predicts mean aerodynamic properties of square prism. In conclusion, this prediction approach can be applied to problems where mean aerodynamic properties are of importance such as galloping problem. On the other hand, further investigation is necessary for prediction of fluctuation properties.

5 ACKNOWLEDGEMENT

We thank Dr. Nishimura, Nihon Architecture Research Institute, for providing us his experiment data for the study.

REFERENCES

1 Ohotsuki, Y., Fujii, K., Washizu, K., Ohya, A. (1978), "Wind tunnel experiments of aerodynamic forces and pressure distributions of rectangular cylinders in a uniform flow (in Japanese)," 5th Symp. on Wind Effects on Structures in Japan, pp.169-176.

2 Nishimura, H, Taniike, Y. (2000), "Fluctuating wind forces on a stationary two-dim square prism," pp. 255-260, 16th Wind Engineering Symposium in Japan.

3 Hirano, H, Maruoka, A, Watanabe, S., (2000), ". Calculation of Aerodynamic Properties of Rectangular Cylinder withSlenderness Ratio of 2:1 under various Angle of Attack, Journal of Structual Engineering, JSCE, Vol.48A, pp. 971- 978, 2002.

4 Tamura, T., Ohta, I., and Kuwahara, K. : On the reiablility of two-dimensional simulation for unsteady flows around a cylinder-type, J. of Wind Eng. and Indus. Aerodyn., vol 35, pp. 275-298, 1990.

5 Nakadou, S., Kimura, K, Fujino, Y., Ogawa, T., Ishihara, T., Characteristics of aerodynamic sound from rectangularcylinder with various side ratios, Journal of structural Mechanics and Earthquake Engineering, JSCE, No.696, I-58, pp.145-155, 2002.

6 Taylor, I., Vezza, M. (1999), Calculation of thee flow field around a square section cylinder undergoing forced transerse oscillations using a discrete vortex, J. of Wind Eng. and Indus. Aerodyn., vol 82, pp.271-291.

7 Asagawa, T., Ishihara, T, Fujino, Y., Numerical Study of Aerodynamic forces and Aeroacoustics of Square prism , JSCE 56th Annual meeting, pp. 766-767, 2001.

8 Smagorinsky, J, General Circulation Experiments with the Primitive Equations. I. The Basic Experiment. Month. Wea. Rev., 91:99-164, 1963.

9 Ma, X., Karamanos, G.-S, and Karniadakis, G.E Dynamics and low-dimensionality of a turbulent near wake, J. Fluid Mech., vol 410, pp. 29-65, 2000.

10 FLUENT 6 Users Guide, Flunet Inc., 2002

11 Hayashi, K., Ohoya, Y., A Numerical Study of The flow Around a Rectangular Cylinder with Critical Depth, 16th Japanese Wind Engineering Symposium Proceeding, pp.179-184, 2000.